CERN-TH/99-175

Heavy quark $1/m_Q$ contributions in semileptonic B decays to orbitally excited D mesons

D. Ebert[1,2], R. N. Faustov[2*] and V. O. Galkin[3]
[1] *Theory Division, CERN, CH-1211 Geneva 23, Switzerland*
[2] *Institut für Physik, Humboldt–Universität zu Berlin, Invalidenstr.110, D-10115 Berlin, Germany*
[3] *Russian Academy of Sciences, Scientific Council for Cybernetics, Vavilov Street 40, Moscow 117333, Russia*

Abstract

Exclusive semileptonic decays of B mesons to orbitally excited D mesons are considered beyond the infinitely heavy quark limit in the framework of the relativistic quark model based on the quasipotential approach. This model agrees with the structure of heavy quark mass corrections predicted by the heavy quark effective theory and allows the determination of corresponding leading and subleading Isgur–Wise functions. It is found that both relativistic and $1/m_Q$ contributions significantly influence the decay rates. Thus, relativistic transformations of the meson wave functions (Wigner rotation of the light quark spin) already contribute at leading order of the heavy quark expansion and result in a suppression of $B \to D_0^* e\nu$ and $B \to D_1^* e\nu$ decay rates. On the other hand, the vanishing of the decay matrix elements at zero recoil of a final D^{**} meson in the infinitely heavy quark mass limit makes the $1/m_Q$ corrections to be very important, and their account results in a substantial enhancement of $B \to D_1 e\nu$ and $B \to D_0^* e\nu$ decay rates.

CERN-TH/99-175
June 1999

---

*On leave of absence from the Russian Academy of Sciences, Scientific Council for Cybernetics, Vavilov Street 40, Moscow 117333, Russia.

I. INTRODUCTION

The investigation of semileptonic decays of B mesons to excited D meson states is an important problem for heavy flavour physics. In particular, these decays can provide an additional source of information for the determination of the Cabibbo–Kobayashi–Maskawa matrix element V_{cb} as well as on the relativistic quark dynamics inside heavy–light mesons. The experimental data on these decays are becoming available now [1–3], and the B factories will provide more accurate and comprehensive data. It is necessary to note that the experiment shows that only approximately 60% of the inclusive semileptonic B decay rate is due to the decays to ground state pseudoscalar D and vector D^* mesons. Thus the rest of these decays should go to excited D meson and continuum states.

The presence of the heavy quark in the initial and final meson states in these decays considerably simplifies their theoretical description. A good starting point for this analysis is the infinitely heavy quark limit, $m_Q \to \infty$ [4]. In this limit the heavy quark symmetry arises, which strongly reduces the number of independent weak form factors [5]. The heavy quark mass and spin then decouple and all meson properties are determined by light-quark degrees of freedom alone. As a result the heavy quark degeneracy of energy levels emerges. The spin s_q of the light quark couples with its orbital momentum l ($j = l \pm s_q$), resulting for P-wave mesons in two degenerate $j = 3/2$ states ($J^P = 1^+, 2^+$)[1] and two degenerate $j = 1/2$ states ($0^+, 1^+$). The heavy quark symmetry also predicts that the form factors for $B \to D^{**} e\nu$ decays, where D^{**} is a generic P-wave D meson state[2], can be expressed in terms of two independent Isgur–Wise functions [5]. However, in the infinitely heavy quark limit the decay matrix elements between a B meson and an orbitally excited D meson vanish at zero recoil because of the heavy quark spin-flavour symmetry [5]. The kinematically allowed range for these decays is not broad. As a result the role of relativistic and finite heavy quark mass contributions not vanishing at zero recoil is considerably more important here than in the decays to ground state D mesons. Thus, the magnitude of such corrections might be comparable with the leading order result.

Recently the first order $1/m_Q$ corrections to the exclusive semileptonic B decays into excited charmed mesons were investigated within the heavy quark effective theory (HQET) [6]. The structure of the $1/m_Q$ corrections to decay matrix elements, which follows from QCD and heavy quark symmetry, was determined. It was found that at the first order of heavy quark expansion the $B \to D_1$, $B \to D_0^*$ and $B \to D_1^*$ matrix elements do not vanish at zero recoil and can be expressed at this kinematical point in terms of the leading Isgur–Wise functions. Away from the zero recoil point new subleading Isgur–Wise functions arise, which cannot be determined from symmetry considerations alone. Thus for their determination, additional model dependent assumptions are necessary. In Ref. [6] an estimation of these functions, based on the non-relativistic quark model as well as on some additional assumptions, was made. It is just here that we can apply the relativistic quark model to get a more

---

[1]Here $J = j \pm 1/2$ is the total angular momentum, and the superscript P denotes the meson parity.

[2]For concrete P-wave meson states the standard notations D_1, D_2^*, D_1^* and D_0^* are used.

consistent calculation of relevant Isgur–Wise functions and decay rates.

Our relativistic quark model is based on the quasipotential approach in quantum field theory with a specific choice of the quark–antiquark interaction potential. It provides a consistent scheme for the calculation of all relativistic corrections at a given v^2/c^2 order and allows for the heavy quark $1/m_Q$ expansion. In preceding papers we applied this model to the calculation of the mass spectra of orbitally and radially excited states of heavy–light mesons [7], as well as to a description of weak decays of B mesons to ground state heavy and light mesons [8,9]. The heavy quark expansion for the ground state heavy-to-heavy semileptonic transitions [10] has been found to be in agreement with model-independent predictions of the HQET. We considered the exclusive semileptonic decays of B mesons to orbitally excited D mesons in the infinitely heavy quark limit in [11] and found the important relativistic contribution to the leading Isgur–Wise functions arising from the relativistic transformation of the meson wave function.

The paper is organized as follows. In Sec. II we briefly present the necessary HQET results on the $B \to D^{**}$ transition matrix elements obtained in Ref. [6]. In Sec. III we describe our relativistic quark model, putting special emphasis on the calculation of decay matrix elements and on the relativistic transformation of a meson wave function from the rest reference frame to the moving one. The heavy quark expansion for decay matrix elements is carried out up to the first order $1/m_Q$ corrections and compared to model independent HQET predictions in Secs. IV-VI. There we present our results for leading and subleading Isgur–Wise functions and compare predictions for decay rates with and without the $1/m_Q$ corrections being taken into account. Taking account of $1/m_Q$ corrections leads to a substantial enhancement of $B \to D_1 e\nu$ and $B \to D_0^* e\nu$ decay rates and gives better agreement between theoretical predictions and available experimental data. We also present the electron spectra for the considered decays and test the fulfilment of the Bjorken sum rule. Section VII contains our conclusions.

II. HQET RESULTS FOR DECAY MATRIX ELEMENTS

A. $B \to D_1 e\nu$ and $B \to D_2^* e\nu$ decays

The matrix elements of the vector and axial-vector currents between B mesons and D_1 or D_2^* mesons can be parametrized in the following way

$$\begin{aligned}
\frac{\langle D_1(v',\epsilon)|\bar{c}\gamma^\mu b|B(v)\rangle}{\sqrt{m_{D_1} m_B}} &= f_{V_1}\epsilon^{*\mu} + (f_{V_2} v^\mu + f_{V_3} v'^\mu)(\epsilon^* \cdot v),\\
\frac{\langle D_1(v',\epsilon)|\bar{c}\gamma^\mu\gamma_5 b|B(v)\rangle}{\sqrt{m_{D_1} m_B}} &= i f_A \varepsilon^{\mu\alpha\beta\gamma}\epsilon^*_\alpha v_\beta v'_\gamma,\\
\frac{\langle D_2^*(v',\epsilon)|\bar{c}\gamma^\mu\gamma_5 b|B(v)\rangle}{\sqrt{m_{D_2^*} m_B}} &= k_{A_1}\epsilon^{*\mu\alpha} v_\alpha + \left(k_{A_2} v^\mu + k_{A_3} v'^\mu\right)\epsilon^*_{\alpha\beta} v^\alpha v^\beta\\
\frac{\langle D_2^*(v',\epsilon)|\bar{c}\gamma^\mu b|B(v)\rangle}{\sqrt{m_{D_2^*} m_B}} &= i k_V \varepsilon^{\mu\alpha\beta\gamma}\epsilon^*_{\alpha\sigma} v^\sigma v_\beta v'_\gamma,
\end{aligned} \tag{1}$$

where v (v') is the four-velocity of the B (D^{**}) meson, ϵ^μ ($\epsilon^{\mu\nu}$) is a polarization vector (tensor) of the final vector (tensor) charmed meson, and the form factors f_i and k_i are

dimensionless functions of $w = v \cdot v'$. The double differential decay rates expressed in terms of the form factors read as follows [5,6]:

$$\begin{aligned}
\frac{\mathrm{d}^2\Gamma_{D_1}}{\mathrm{d}w\mathrm{d}\cos\theta} &= 3\Gamma_0 r_1^3\sqrt{w^2-1}\Big\{\sin^2\theta\Big[(w-r_1)f_{V_1}+(w^2-1)(f_{V_3}+r_1 f_{V_2})\Big]^2 \\
&\quad +(1-2r_1w+r_1^2)\Big[(1+\cos^2\theta)[f_{V_1}^2+(w^2-1)f_A^2]-4\cos\theta\sqrt{w^2-1}f_{V_1}f_A\Big]\Big\}, \\
\frac{\mathrm{d}^2\Gamma_{D_2^*}}{\mathrm{d}w\mathrm{d}\cos\theta} &= \frac{3}{2}\Gamma_0 r_2^3(w^2-1)^{3/2}\Big\{\frac{4}{3}\sin^2\theta\Big[(w-r_2)k_{A_1}+(w^2-1)(k_{A_3}+r_2k_{A_2})\Big]^2 \\
&\quad +(1-2r_2w+r_2^2)\Big[(1+\cos^2\theta)[k_{A_1}^2+(w^2-1)k_V^2]-4\cos\theta\sqrt{w^2-1}k_{A_1}k_V\Big]\Big\}, \quad (2)
\end{aligned}$$

where $\Gamma_0 = G_F^2\,|V_{cb}|^2\,m_B^5/(192\pi^3)$, $r_1 = m_{D_1}/m_B$, $r_2 = m_{D_2^*}/m_B$, and θ is the angle between the charged lepton and the charmed meson in the rest frame of the virtual W boson.

The main predictions of HQET for the structure of the $B \to D_1 e\nu$ form factors look as follows [6]:

$$\begin{aligned}
\sqrt{6}f_A &= -(w+1)\tau - \varepsilon_b\{(w-1)[(\bar\Lambda'+\bar\Lambda)\tau-(2w+1)\tau_1-\tau_2]+(w+1)\eta_b\} \\
&\quad -\varepsilon_c[4(w\bar\Lambda'-\bar\Lambda)\tau-3(w-1)(\tau_1-\tau_2)+(w+1)(\eta_{\rm ke}-2\eta_1-3\eta_3)], \\
\sqrt{6}f_{V_1} &= (1-w^2)\tau - \varepsilon_b(w^2-1)[(\bar\Lambda'+\bar\Lambda)\tau-(2w+1)\tau_1-\tau_2+\eta_b] \\
&\quad -\varepsilon_c[4(w+1)(w\bar\Lambda'-\bar\Lambda)\tau-(w^2-1)(3\tau_1-3\tau_2-\eta_{\rm ke}+2\eta_1+3\eta_3)], \\
\sqrt{6}f_{V_2} &= -3\tau - 3\varepsilon_b[(\bar\Lambda'+\bar\Lambda)\tau-(2w+1)\tau_1-\tau_2+\eta_b] \\
&\quad -\varepsilon_c[(4w-1)\tau_1+5\tau_2+3\eta_{\rm ke}+10\eta_1+4(w-1)\eta_2-5\eta_3], \\
\sqrt{6}f_{V_3} &= (w-2)\tau + \varepsilon_b\{(2+w)[(\bar\Lambda'+\bar\Lambda)\tau-(2w+1)\tau_1-\tau_2]-(2-w)\eta_b\} \\
&\quad +\varepsilon_c[4(w\bar\Lambda'-\bar\Lambda)\tau+(2+w)\tau_1+(2+3w)\tau_2+(w-2)\eta_{\rm ke} \\
&\quad -2(6+w)\eta_1-4(w-1)\eta_2-(3w-2)\eta_3], \qquad (3)
\end{aligned}$$

where $\varepsilon_Q = 1/(2m_Q)$ and $\bar\Lambda(\bar\Lambda') = M(M') - m_Q$ is the difference between the heavy ground state (orbitally excited) meson and heavy quark masses in the limit $m_Q \to \infty$. The form factor τ is the leading order Isgur–Wise function (τ is $\sqrt{3}$ times the function τ_{32} of Refs. [5,11]). The subleading Isgur–Wise functions τ_1 and τ_2 originate from the $1/m_Q$ corrections to the $b \to c$ flavour changing current, while η_{ke} and η_i form factors result from kinetic energy and chromomagnetic corrections to the HQET Lagrangian.

The analogous formulae for $B \to D_2^* e\nu$ have the form [6]

$$\begin{aligned}
k_V &= -\tau - \varepsilon_b[(\bar\Lambda'+\bar\Lambda)\tau-(2w+1)\tau_1-\tau_2+\eta_b]-\varepsilon_c(\tau_1-\tau_2+\eta_{\rm ke}-2\eta_1+\eta_3), \\
k_{A_1} &= -(1+w)\tau - \varepsilon_b\{(w-1)[(\bar\Lambda'+\bar\Lambda)\tau-(2w+1)\tau_1-\tau_2]+(1+w)\eta_b\}
\end{aligned}$$

$$-\varepsilon_c[(w-1)(\tau_1-\tau_2)+(w+1)(\eta_{\rm ke}-2\eta_1+\eta_3)],$$

$$k_{A_2}=-2\varepsilon_c(\tau_1+\eta_2),$$

$$k_{A_3}=\tau+\varepsilon_b[(\bar\Lambda'+\bar\Lambda)\tau-(2w+1)\tau_1-\tau_2+\eta_b]-\varepsilon_c(\tau_1+\tau_2-\eta_{\rm ke}+2\eta_1-2\eta_2-\eta_3). \quad (4)$$

B. $B\to D_0^* e\nu$ and $B\to D_1^* e\nu$ decays

The matrix elements of the vector and axial currents between B mesons and D_0^* or D_1^* mesons can be parametrized as follows

$$\begin{aligned}
\langle D_0^*(v')|\bar c\gamma^\mu b|B(v)\rangle &= 0,\\
\frac{\langle D_0^*(v')|\bar c\gamma^\mu\gamma_5 b|B(v)\rangle}{\sqrt{m_{D_0^*}m_B}} &= g_+(v^\mu+v'^\mu)+g_-(v^\mu-v'^\mu),\\
\frac{\langle D_1^*(v',\epsilon)|\bar c\gamma^\mu b|B(v)\rangle}{\sqrt{m_{D_1^*}m_B}} &= g_{V_1}\epsilon^{*\mu}+(g_{V_2}v^\mu+g_{V_3}v'^\mu)\,(\epsilon^*\cdot v),\\
\frac{\langle D_1^*(v',\epsilon)|\bar c\gamma^\mu\gamma_5 b|B(v)\rangle}{\sqrt{m_{D_1^*}m_B}} &= ig_A\varepsilon^{\mu\alpha\beta\gamma}\epsilon^*_\alpha v_\beta v'_\gamma,
\end{aligned} \quad (5)$$

where the form factors g_i are functions of w. In terms of these form factors the double differential decay rates for $B\to D_0^*\,e\,\bar\nu_e$ and $B\to D_1^*\,e\,\bar\nu_e$ decays can be expressed in the following way [6]

$$\begin{aligned}
\frac{{\rm d}^2\Gamma_{D_0^*}}{{\rm d}w{\rm d}\cos\theta} &= 3\Gamma_0 r_0^{*3}\,(w^2-1)^{3/2}\sin^2\theta\Big[(1+r_0^*)g_+-(1-r_0^*)g_-\Big]^2,\\
\frac{{\rm d}^2\Gamma_{D_1^*}}{{\rm d}w{\rm d}\cos\theta} &= 3\Gamma_0 r_1^{*3}\sqrt{w^2-1}\Big\{\sin^2\theta\Big[(w-r_1^*)g_{V_1}+(w^2-1)(g_{V_3}+r_1^*g_{V_2})\Big]^2\\
&\quad+(1-2r_1^*w+r_1^{*2})\Big[(1+\cos^2\theta)[g_{V_1}^2+(w^2-1)g_A^2]-4\cos\theta\sqrt{w^2-1}g_{V_1}g_A\Big]\Big\},
\end{aligned} \quad (6)$$

where $\Gamma_0=G_F^2\,|V_{cb}|^2\,m_B^5/(192\pi^3)$, $r_0^*=m_{D_0^*}/m_B$ and $r_1^*=m_{D_1^*}/m_B$.

The HQET predictions for the form factors of the decay $B\to D_0^* e\nu$ are given by [6]

$$\begin{aligned}
g_+ &= \varepsilon_c\left[2(w-1)\zeta_1-3\zeta\frac{w\bar\Lambda^*-\bar\Lambda}{w+1}\right]-\varepsilon_b\left[\frac{\bar\Lambda^*(2w+1)-\bar\Lambda(w+2)}{w+1}\zeta-2(w-1)\zeta_1\right],\\
g_- &= \zeta+\varepsilon_c\,[\chi_{\rm ke}+6\chi_1-2(w+1)\chi_2]+\varepsilon_b\chi_b.
\end{aligned} \quad (7)$$

The analogous formulae for the decay $B\to D_1^* e\nu$ look as follows

$$\begin{aligned}
g_A &= \zeta+\varepsilon_c\left[\frac{w\bar\Lambda^*-\bar\Lambda}{w+1}\zeta+\chi_{\rm ke}-2\chi_1\right]-\varepsilon_b\left[\frac{\bar\Lambda^*(2w+1)-\bar\Lambda(w+2)}{w+1}\zeta-2(w-1)\zeta_1-\chi_b\right],\\
g_{V_1} &= (w-1)\zeta+\varepsilon_c\Big[(w\bar\Lambda^*-\bar\Lambda)\zeta+(w-1)(\chi_{\rm ke}-2\chi_1)\Big]
\end{aligned}$$

$$-\varepsilon_b \left\{ [\bar\Lambda^*(2w+1) - \bar\Lambda(w+2)]\zeta - 2(w^2-1)\zeta_1 - (w-1)\chi_b \right\},$$

$$g_{V_2} = 2\varepsilon_c(\zeta_1 - \chi_2),$$

$$g_{V_3} = -\zeta - \varepsilon_c \left[\frac{w\bar\Lambda^* - \bar\Lambda}{w+1}\zeta + 2\zeta_1 + \chi_{\rm ke} - 2\chi_1 + 2\chi_2 \right]$$
$$+\varepsilon_b \left[\frac{\bar\Lambda^*(2w+1) - \bar\Lambda(w+2)}{w+1}\zeta - 2(w-1)\zeta_1 - \chi_b \right]. \qquad (8)$$

The form factor ζ is the leading order Isgur–Wise function (ζ is twice the function τ_{12} of Refs. [5,11]). The subleading Isgur–Wise function ζ_1 originates from the $1/m_Q$ corrections to the $b \to c$ flavour changing current, while χ_{ke} and χ_i form factors result from kinetic energy and chromomagnetic corrections to the HQET Lagrangian.

In the following sections we apply the relativistic quark model to the calculation of leading and subleading Isgur–Wise functions.

III. RELATIVISTIC QUARK MODEL

In the quasipotential approach, a meson is described by the wave function of the bound quark–antiquark state, which satisfies the quasipotential equation [12] of the Schrödinger type [13]:

$$\left(\frac{b^2(M)}{2\mu_R} - \frac{\mathbf{p}^2}{2\mu_R} \right) \Psi_M(\mathbf{p}) = \int \frac{d^3q}{(2\pi)^3} V(\mathbf{p},\mathbf{q};M)\Psi_M(\mathbf{q}), \qquad (9)$$

where the relativistic reduced mass is

$$\mu_R = \frac{M^4 - (m_q^2 - m_Q^2)^2}{4M^3}. \qquad (10)$$

Here $m_{q,Q}$ are the masses of light and heavy quarks, and $\mathbf{p}$ is their relative momentum. In the centre-of-mass system the relative momentum squared on mass shell reads

$$b^2(M) = \frac{[M^2 - (m_q + m_Q)^2][M^2 - (m_q - m_Q)^2]}{4M^2}. \qquad (11)$$

The kernel $V(\mathbf{p},\mathbf{q};M)$ in Eq. (9) is the quasipotential operator of the quark–antiquark interaction. It is constructed with the help of the off-mass-shell scattering amplitude, projected onto the positive energy states. An important role in this construction is played by the Lorentz-structure of the confining quark–antiquark interaction in the meson. In constructing the quasipotential of the quark-antiquark interaction we have assumed that the effective interaction is the sum of the usual one-gluon exchange term and the mixture of vector and scalar linear confining potentials. The quasipotential is then defined by [14]

$$V(\mathbf{p},\mathbf{q};M) = \bar u_q(p)\bar u_Q(-p)\mathcal{V}(\mathbf{p},\mathbf{q};M)u_q(q)u_Q(-q)$$
$$= \bar u_q(p)\bar u_Q(-p)\left\{ \frac{4}{3}\alpha_s D_{\mu\nu}(\mathbf{k})\gamma_q^\mu\gamma_Q^\nu \right.$$

$$+V^V_{\rm conf}(\mathbf{k})\Gamma^\mu_q\Gamma_{Q;\mu}+V^S_{\rm conf}(\mathbf{k})\Big\}u_q(q)u_Q(-q), \tag{12}$$

where α_s is the QCD coupling constant, $D_{\mu\nu}$ is the gluon propagator in the Coulomb gauge and $\mathbf{k}=\mathbf{p}-\mathbf{q}$; γ_μ and $u(p)$ are the Dirac matrices and spinors

$$u^\lambda(p)=\sqrt{\frac{\epsilon(p)+m}{2\epsilon(p)}}\begin{pmatrix}1\\ \frac{\boldsymbol{\sigma p}}{\epsilon(p)+m}\end{pmatrix}\chi^\lambda \tag{13}$$

with $\epsilon(p)=\sqrt{\mathbf{p}^2+m^2}$. The effective long-range vector vertex is given by

$$\Gamma_\mu(\mathbf{k})=\gamma_\mu+\frac{i\kappa}{2m}\sigma_{\mu\nu}k^\nu, \tag{14}$$

where κ is the Pauli interaction constant characterizing the anomalous chromomagnetic moment of quarks. Vector and scalar confining potentials in the non-relativistic limit reduce to

$$V^V_{\rm conf}(r)=(1-\varepsilon)(Ar+B),\qquad V^S_{\rm conf}(r)=\varepsilon(Ar+B), \tag{15}$$

reproducing

$$V_{\rm conf}(r)=V^S_{\rm conf}(r)+V^V_{\rm conf}(r)=Ar+B, \tag{16}$$

where ε is the mixing coefficient.

The quasipotential for the heavy quarkonia, expanded in v^2/c^2, can be found in Refs. [14,15] and for heavy–light mesons in [7]. All the parameters of our model, such as quark masses, parameters of the linear confining potential, mixing coefficient ε and anomalous chromomagnetic quark moment κ, were fixed from the analysis of heavy quarkonia masses [14] and radiative decays [16]. The quark masses $m_b=4.88$ GeV, $m_c=1.55$ GeV, $m_s=0.50$ GeV, $m_{u,d}=0.33$ GeV and the parameters of the linear potential $A=0.18$ GeV^2 and $B=-0.30$ GeV have usual quark model values. The value of the vector-scalar mixing coefficient $\varepsilon=-1$ has been determined by considering the heavy quark expansion [10] and meson radiative decays [16]. Finally, the universal Pauli interaction constant $\kappa=-1$ has been fixed from the analysis of the fine splitting of heavy quarkonia ^3P_J- states [14]. Note that the long-range magnetic contribution to the potential in our model is proportional to $(1+\kappa)$ and thus vanishes for the chosen value of $\kappa=-1$.

In order to calculate the exclusive semileptonic decay rate of the B meson, it is necessary to determine the corresponding matrix element of the weak current between meson states. In the quasipotential approach, the matrix element of the weak current $J^W=\bar c\gamma_\mu(1-\gamma^5)b$ between a B meson and an orbitally excited D^{**} meson takes the form [17]

$$\langle D^{**}|J^W_\mu(0)|B\rangle=\int\frac{d^3p\,d^3q}{(2\pi)^6}\bar\Psi_{D^{**}}(\mathbf{p})\Gamma_\mu(\mathbf{p},\mathbf{q})\Psi_B(\mathbf{q}), \tag{17}$$

where $\Gamma_\mu(\mathbf{p},\mathbf{q})$ is the two-particle vertex function and $\Psi_{B,D^{**}}$ are the meson wave functions projected onto the positive energy states of quarks and boosted to the moving reference

frame. The contributions to Γ come from Figs. 1 and 2.[3] In the heavy quark limit $m_{b,c} \to \infty$ only $\Gamma^{(1)}$ contributes, while $\Gamma^{(2)}$ contributes at $1/m_Q$ order. They look like

$$\Gamma^{(1)}(\mathbf{p},\mathbf{q}) = \bar{u}_c(p_c)\gamma_\mu(1-\gamma^5)u_b(q_b)(2\pi)^3\delta(\mathbf{p}_q-\mathbf{q}_q), \tag{18}$$

and

$$\Gamma^{(2)}(\mathbf{p},\mathbf{q}) = \bar{u}_c(p_c)\bar{u}_q(p_q)\Big\{\gamma_\mu(1-\gamma^5)\frac{\Lambda_b^{(-)}(k)}{\epsilon_b(k)+\epsilon_b(p_c)}\gamma_1^0\mathcal{V}(\mathbf{p}_q-\mathbf{q}_q) + \mathcal{V}(\mathbf{p}_q-\mathbf{q}_q)\frac{\Lambda_c^{(-)}(k')}{\epsilon_c(k')+\epsilon_c(q_b)}\gamma_1^0\gamma_\mu(1-\gamma^5)\Big\}u_b(q_b)u_q(q_q), \tag{19}$$

where the superscripts "(1)" and "(2)" correspond to Figs. 1 and 2, $\mathbf{k} = \mathbf{p}_c - \mathbf{\Delta}$; $\mathbf{k}' = \mathbf{q}_b + \mathbf{\Delta}$; $\mathbf{\Delta} = \mathbf{p}_B - \mathbf{p}_{D^{**}}$; $\epsilon(p) = (m^2+\mathbf{p}^2)^{1/2}$;

$$\Lambda^{(-)}(p) = \frac{\epsilon(p) - (m\gamma^0 + \gamma^0(\boldsymbol{\gamma}\boldsymbol{p}))}{2\epsilon(p)}.$$

Here [17]

$$p_{c,q} = \epsilon_{c,q}(p)\frac{p_{D^{**}}}{M_{D^{**}}} \pm \sum_{i=1}^{3} n^{(i)}(p_{D^{**}})p^i,$$
$$q_{b,q} = \epsilon_{b,q}(p)\frac{p_B}{M_B} \pm \sum_{i=1}^{3} n^{(i)}(p_B)q^i,$$

and $n^{(i)}$ are three four-vectors given by

$$n^{(i)\mu}(p) = \left\{\frac{p^i}{M},\ \delta_{ij} + \frac{p^i p^j}{M(E+M)}\right\}.$$

The wave function of a P-wave D^{**} meson at rest is given by

$$\Psi_{D^{**}}(\mathbf{p}) \equiv \Psi^{JM}_{D(j)}(\mathbf{p}) = \mathcal{Y}^{JM}_j \psi_{D(j)}(\mathbf{p}), \tag{20}$$

where J and M are the total meson angular momentum and its projection, while j is the light quark angular momentum; $\psi_{D(j)}(\mathbf{p})$ is the radial part of the wave function, which has been determined by the numerical solution of Eq. (9) in [7]. The spin-angular momentum part $\mathcal{Y}^{JM}_j$ has the following form

$$\mathcal{Y}^{JM}_j = \sum_{\sigma_Q\sigma_q}\left\langle j\ M-\sigma_Q,\ \frac{1}{2}\,\sigma_Q|J\ M\right\rangle\left\langle 1\ M-\sigma_Q-\sigma_q,\ \frac{1}{2}\,\sigma_q|j\ M-\sigma_Q\right\rangle \times Y_1^{M-\sigma_Q-\sigma_q}\chi_Q(\sigma_Q)\chi_q(\sigma_q). \tag{21}$$

---

[3]The contribution $\Gamma^{(2)}$ is the consequence of the projection onto the positive-energy states. Note that the form of the relativistic corrections resulting from the vertex function $\Gamma^{(2)}$ is explicitly dependent on the Lorentz structure of the $q\bar{q}$-interaction.

Here $\langle j_1\, m_1,\ j_2\, m_2 | J\, M\rangle$ are Clebsch-Gordan coefficients, Y_l^m are spherical harmonics, and $\chi(\sigma)$ (where $\sigma = \pm 1/2$) are spin wave functions :

$$\chi\,(1/2) = \begin{pmatrix}1\\0\end{pmatrix}, \qquad \chi\,(-1/2) = \begin{pmatrix}0\\1\end{pmatrix}.$$

It is important to note that the wave functions entering the weak current matrix element (17) are not in the rest frame in general. For example, in the B meson rest frame, the D^{**} meson is moving with the recoil momentum $\mathbf{\Delta}$. The wave function of the moving D^{**} meson $\Psi_{D^{**}\,\mathbf{\Delta}}$ is connected with the D^{**} wave function in the rest frame $\Psi_{D^{**}\,\mathbf{0}} \equiv \Psi_{D(j)}$ by the transformation [17]

$$\Psi_{D^{**}\,\mathbf{\Delta}}(\mathbf{p}) = D_c^{1/2}(R^W_{L\mathbf{\Delta}}) D_q^{1/2}(R^W_{L\mathbf{\Delta}}) \Psi_{D^{**}\,\mathbf{0}}(\mathbf{p}), \tag{22}$$

where R^W is the Wigner rotation and the rotation matrix $D^{1/2}(R)$ in spinor representation is given by

$$\begin{pmatrix}1 & 0\\ 0 & 1\end{pmatrix} D^{1/2}_{c,q}(R^W_{L\mathbf{\Delta}}) = S^{-1}(\mathbf{p}_{c,q}) S(\mathbf{\Delta}) S(\mathbf{p}), \tag{23}$$

where

$$S(\mathbf{p}) = \sqrt{\frac{\epsilon(p)+m}{2m}} \left(1 + \frac{\boldsymbol{\alpha p}}{\epsilon(p)+m}\right)$$

is the usual Lorentz transformation matrix of the four-spinor. For electroweak B meson decays to S-wave final mesons such a transformation contributes at first order of the $1/m_Q$ expansion, while for the decays to excited final mesons it gives a contribution already to the leading term due to the orthogonality of the initial and final meson wave functions.

IV. LEADING AND SUBLEADING ISGUR–WISE FUNCTIONS

Now we can perform the heavy quark expansion for the matrix elements of B decays to orbitally excited D mesons in the framework of our model and determine leading and subleading Isgur–Wise functions. We substitute the vertex functions $\Gamma^{(1)}$ and $\Gamma^{(2)}$ given by Eqs. (18) and (19) in the decay matrix element (17) and take into account the wave function properties (20)–(22). [4] The resulting structure of this matrix element is rather complicated, because it is necessary to integrate both over d^3p and d^3q. The δ function in expression (18) permits us to perform one of these integrations and thus this contribution can be easily calculated. The calculation of the vertex function $\Gamma^{(2)}$ contribution is more difficult. Here, instead of a δ function, we have a complicated structure, containing the $Q\bar{q}$ interaction potential in the meson. However, we can expand this contribution in inverse powers of heavy (b, c) quark masses and then use the quasipotential equation in order to perform one

[4] Note that the quark model definition of $\Psi_{D_1^*(1/2)}$ in (20), (21) differs from the HQET one [5,6] by an overall minus sign.

of the integrations in the current matrix element. We carry out the heavy quark expansion up to first order in $1/m_Q$. It is easy to see that the vertex function $\Gamma^{(2)}$ contributes already at the subleading order of the $1/m_Q$ expansion. Then we compare the arising decay matrix elements with the form factor decompositions (1) and (5) and determine the corresponding form factors. We find that, for the chosen values of our model parameters (the mixing coefficient of vector and scalar confining potential $\varepsilon = -1$ and the Pauli constant $\kappa = -1$), the resulting structure at leading and subleading order in $1/m_Q$ coincides with the model-independent predictions of HQET given by Eqs. (3), (4), (7), and (8). We get the following expressions for leading and subleading Isgur–Wise functions:

i) $B \to D_1 e\nu$ and $B \to D_2^* e\nu$ decays

$$\tau(w) = \sqrt{\frac{2}{3}}\frac{1}{(w+1)^{3/2}}\int\frac{d^3p}{(2\pi)^3}\bar\psi_{D(3/2)}\left(\mathbf{p}+\frac{2\epsilon_q}{M_{D(3/2)}(w+1)}\mathbf{\Delta}\right) \times\left[-2\epsilon_q\frac{\overleftarrow{\partial}}{\partial p}+\frac{p}{\epsilon_q+m_q}\right]\psi_B(\mathbf{p}), \tag{24}$$

$$\tau_1(w) = \frac{\bar\Lambda'+\bar\Lambda}{w+1}\tau(w), \tag{25}$$

$$\tau_2(w) = -\frac{w}{w+1}(\bar\Lambda'+\bar\Lambda)\tau(w). \tag{26}$$

ii) $B \to D_0^* e\nu$ and $B \to D_1^* e\nu$ decays

$$\zeta(w) = \frac{\sqrt{2}}{3}\frac{1}{(w+1)^{1/2}}\int\frac{d^3p}{(2\pi)^3}\bar\psi_{D(1/2)}\left(\mathbf{p}+\frac{2\epsilon_q}{M_{D(1/2)}(w+1)}\mathbf{\Delta}\right) \times\left[-2\epsilon_q\frac{\overleftarrow{\partial}}{\partial p}-\frac{2p}{\epsilon_q+m_q}\right]\psi_B(\mathbf{p}), \tag{27}$$

$$\zeta_1(w) = \frac{\bar\Lambda^*+\bar\Lambda}{w+1}\zeta(w). \tag{28}$$

The contributions of all other subleading form factors, $\eta_i(w)$ and $\chi_i(w)$, to decay matrix elements are suppressed by an additional power of the ratio $(w-1)/(w+1)$, which is equal to zero at $w=1$ and less than $1/6$ at $w_{\max} = (1+r^2)/(2r)$ ($r = r_1, r_2, r_0^*$, or r_1^* respectively). Since the main contribution to the decay rate comes from the values of form factors close to $w=1$, these form factors turn out to be unimportant. This result is in agreement with the HQET-motivated considerations [6] that the functions parametrizing the time-ordered products of the chromomagnetic term in the HQET Lagrangian with the leading order currents should be small.

The arrow over $\partial/\partial p$ in (24) and (27) indicates that the derivative acts on the wave function of the D^{**} meson. All the wave functions and meson masses have been obtained in [7] by the numerical solution of the quasipotential equation. We use the following values for HQET parameters $\bar\Lambda = 0.51$ GeV, $\bar\Lambda' = 0.80$ GeV, and $\bar\Lambda^* = 0.89$ GeV [7].

The last terms in the square brackets of the expressions for the leading order Isgur–Wise functions $\tau(w)$ (24) and $\zeta(w)$ (27) result from the wave function transformation (22) associated with the relativistic rotation of the light quark spin (Wigner rotation) in passing to the moving reference frame. These terms are numerically important and lead to the

suppression of the ζ form factor compared to τ. Note that if we had applied a simplified non-relativistic quark model [5,18] these important contributions would be missing. Neglecting further the small difference between the wave functions $\psi_{D(1/2)}$ and $\psi_{D(3/2)}$, the following relation between τ and ζ would have been obtained [6]

$$\zeta(w) = \frac{w+1}{\sqrt{3}}\tau(w). \tag{29}$$

However, we see that this relation is violated if the relativistic transformation properties of the wave function are taken into account. At the point $w = 1$, where the initial B meson and final D^{**} are at rest, we find instead the relation

$$\frac{\tau(1)}{\sqrt{3}} - \frac{\zeta(1)}{2} \cong \frac{1}{2}\int \frac{d^3p}{(2\pi)^3}\bar{\psi}_{D^{**}}(\mathbf{p})\frac{p}{\epsilon_q + m_q}\psi_B(\mathbf{p}), \tag{30}$$

obtained by assuming $\psi_{D(3/2)} \cong \psi_{D(1/2)} \cong \psi_{D^{**}}$. The relation (30) coincides with the one found in Ref. [19], where the Wigner rotation was also taken into account.

V. NUMERICAL RESULTS AND PREDICTIONS

In Table I we present our numerical results for the leading order Isgur–Wise functions $\tau(1)$ and $\zeta(1)$ at zero recoil of the final D^{**} meson, as well as their slopes $\rho^2_{3/2} = -\frac{1}{\tau}\frac{\partial}{\partial w}\tau\Big|_{w=1}$ and $\rho^2_{1/2} = -\frac{1}{\zeta}\frac{\partial}{\partial w}\zeta\Big|_{w=1}$, in comparison with other model predictions [6,19–24]. We see that most of the above approaches predict close values for the function $\tau(1)$ and its slope $\rho^2_{3/2}$, while the results for $\zeta(1)$ significantly differ from one another. This difference is a consequence of a specific treatment of the relativistic quark dynamics. Non-relativistic approaches predict $\zeta(1) \simeq (2/\sqrt{3})\tau(1)$ (see (29)), while the relativistic treatment leads to $(2/\sqrt{3})\tau(1) > \zeta(1)$ (see Eq. (30)). The more relativistic the light quark in the heavy–light meson is, the more suppressed ζ is with respect to τ. We plot our results for leading ($\tau(w)$, $\zeta(w)$) and subleading ($\tau_1(w)$, $\tau_2(w)$, $\zeta_1(w)$) Isgur–Wise functions for $B \to D^{**}e\nu$ in Figs. 3, 4 and for $B_s \to D_s^{**}e\nu$ in Figs. 5, 6.

We can now calculate the decay branching ratios by integrating double differential decay rates in Eqs. (2) and (6). Our results for decay rates both in the infinitely heavy quark limit and taking account of the first order $1/m_Q$ corrections as well as their ratio

$$R = \frac{\mathrm{Br}(B \to D^{**}e\nu)_{\text{with } 1/m_Q}}{\mathrm{Br}(B \to D^{**}e\nu)_{m_Q \to \infty}}$$

are presented in Tables II and III. We see that the inclusion of $1/m_Q$ corrections considerably influences the results and for some decays their contribution is as important as the leading order contribution. This is the consequence of the vanishing of the leading order contribution to the decay matrix elements due to the heavy quark spin-flavour symmetry at zero recoil of the final D^{**} meson, while nothing prevents $1/m_Q$ corrections to contribute to the decay matrix element at this kinematical point. In fact, from Eqs. (1) and (5), we see that decay matrix elements at zero recoil are determined by form factors $f_{V_1}(1)$, $g_+(1)$ and $g_{V_1}(1)$,

which receive non-vanishing contributions from first order heavy quark mass corrections. From Eqs. (3), (7), and (8) we find

$$\sqrt{6} f_{V_1}(1) = -8\varepsilon_c(\bar{\Lambda}' - \bar{\Lambda})\tau(1) \tag{31}$$

$$g_+(1) = -\frac{3}{2}(\varepsilon_c + \varepsilon_b)(\bar{\Lambda}^* - \bar{\Lambda})\zeta(1) \tag{32}$$

$$g_{V_1}(1) = (\varepsilon_c - 3\varepsilon_b)(\bar{\Lambda}^* - \bar{\Lambda})\zeta(1). \tag{33}$$

Since the kinematically allowed range for these decays is not broad ($1 \le w \le w_{\max} \approx 1.32$), the contribution to the decay rate of the rather small $1/m_Q$ corrections is substantially increased. This is confirmed by numerical calculations. From Tables II and III we see that the decay rate $B \to D_2^* e\nu$, for which all contributions vanish at zero recoil, is only slightly increased by subleading $1/m_Q$ corrections. On the other hand, $B \to D_1 e\nu$ and $B \to D_0^* e\nu$ decay rates receive large $1/m_Q$ contributions. The situation is different for the $B \to D_1^* e\nu$ decay. Here the $1/m_Q$ contribution at zero recoil is not equal to zero, but it is suppressed by a very small factor $(\varepsilon_c - 3\varepsilon_b)$ (see Eq. (33)), which is only ≈ 0.03 GeV^{-1} for our model parameters. As a result the $B \to D_1^* e\nu$ decay rate receives $1/m_Q$ contributions comparable to those for the $B \to D_2^* e\nu$ rate. The above discussion shows that the sharp increase of $B \to D_1 e\nu$ and $B \to D_0^*$ decay rates by first order $1/m_Q$ corrections does not signal the breakdown of the heavy quark expansion, but is rather a result of the interplay of kinematical and dynamical effects. Thus we have good reasons to expect that higher order $1/m_Q$ corrections will influence these decay rates at the level of 10 – 20 %.

In Table II we present the experimental data from CLEO [1] and ALEPH [2], which are available only for the $B \to D_1 e\nu$ decay. For $B \to D_2^* e\nu$, these experimental groups present only upper limits, which require the use of some additional assumptions about the hadronic branching ratios of the D_2^* meson. Our result for the branching ratio of the $B \to D_1 e\nu$ decay with the inclusion of $1/m_Q$ corrections is in good agreement with both measurements. On the other hand, our branching ratio for the $B \to D_2^* e\nu$ decay is only within the CLEO upper limit and disagrees with the ALEPH one. However, there are some reasons to expect that the ALEPH bound is too strong [6].

In Table IV we present our predictions for the ratios of decay rates $B \to D_2^* e\nu$, $B \to D_0^* e\nu$, $B \to D_1^* e\nu$, and of the sum of all $B \to D^{**} e\nu$ decay rates to the rate $B \to D_1 e\nu$ both in the limit $m_Q \to \infty$, and taking into account the $1/m_Q$ corrections. It is reasonable to consider such ratios in order to normalize to a measured rate. In Ref. [19] it is argued that a ratio $\mathrm{Br}(B \to D_2^* e\nu)/\mathrm{Br}(B \to D_1 e\nu) = 1.55 \pm 0.15$ is a mere consequence of the heavy quark symmetry. In the heavy quark limit we confirm this result. However, the inclusion of $1/m_Q$ corrections strongly influences this prediction and considerably reduce this ratio to a value close to 1. Such a reduction seems to be favoured by available experimental data. In the last row of Table IV we give the sum of all $B \to D^{**} e\nu$ branching ratios. We see that our model predicts that 1.45% of B meson decays go to the first orbitally excited D meson states. This result means that approximately 2.5% of B decays should go to higher excitations.

In Fig. 7 we plot the electron spectra $(1/\Gamma_0)(\mathrm{d}\Gamma/\mathrm{d}y)$ for $B \to D^{**} e\nu$ decays. Here $y = 2E_e/m_B$ is the rescaled lepton energy. These differential decay rates can be easily obtained from double differential decay rates (2), (6), using the relation $y = 1 - rw - r\sqrt{w^2-1}\cos\theta$ and then integrating in w over $[(1-y)^2 + r^2]/[2r(1-y)] < w < (1+r^2)/(2r)$. We present

our results both in the heavy quark limit $m_Q \to \infty$ (dashed curves) and with the inclusion of first order $1/m_Q$ corrections (solid curves).

VI. BJORKEN SUM RULE

Finally we test the fulfilment of the Bjorken sum rule [25] in our model. This sum rule states

$$\rho^2 = \frac{1}{4} + \sum_m \frac{|\zeta^{(m)}(1)|^2}{4} + 2\sum_m \frac{|\tau^{(m)}(1)|^2}{3} + \cdots, \tag{34}$$

where ρ^2 is the slope of the $B \to D^{(*)}e\nu$ Isgur–Wise function, $\zeta^{(m)}$ and $\tau^{(m)}$ are the form factors describing the orbitally excited states discussed here and their radial excitations, and ellipses denote contributions from non-resonant channels. We see that the contribution of the lowest lying P-wave states implies the bound

$$\rho^2 > \frac{1}{4} + \frac{|\zeta(1)|^2}{4} + 2\frac{|\tau(1)|^2}{3} = 0.81, \tag{35}$$

which is in agreement with the slope $\rho^2 = 1.02$ in our model [10] and with experimental values [26].

VII. CONCLUSIONS

In this paper we have applied the relativistic quark model to the consideration of semileptonic B decays to orbitally excited charmed mesons, in the leading and subleading order of the heavy quark expansion. We have found an interesting interplay of the relativistic and finite heavy quark mass contributions. In particular, it has been found that the Lorentz transformation properties of meson wave functions play an important role in the theoretical description of these decays. Thus, the Wigner rotation of the light quark spin gives a significant contribution already at the leading order of the heavy quark expansion. This contribution considerably reduces the leading order Isgur–Wise function ζ with respect to τ. As a result, in this limit, the decay rates $B \to D_0^* e\nu$ and $B \to D_1^* e\nu$ are approximately an order of magnitude smaller than the decay rates $B \to D_1 e\nu$ and $B \to D_2^* e\nu$. On the other hand, inclusion of the first order $1/m_Q$ corrections also substantially influences the decay rates. This large effect of subleading heavy quark corrections is a consequence of the vanishing of the leading order contributions to the decay matrix elements due to heavy quark spin-flavour symmetry at the point of zero recoil of the final charmed meson. However, the subleading order contributions to $B \to D_1 e\nu$, $B \to D_0^* e\nu$ and $B \to D_1^* e\nu$ do not vanish at this kinematical point. Since the kinematical range for these decays is rather small, the role of these corrections is considerably increased. Their account results in an approximately twofold enhancement of the $B \to D_1 e\nu$ and $B \to D_0^* e\nu$ decay rates, while the $B \to D_2^* e\nu$ and $B \to D_1^* e\nu$ rates are increased only slightly. The small influence of $1/m_Q$ corrections on the $B \to D_1^* e\nu$ decay rate is the consequence of the additional interplay of $1/m_c$ and $1/m_b$ corrections at the zero recoil point (see Eq. (33)). We thus see that these subleading heavy quark corrections turn out to be very important and considerably

change the infinitely heavy quark limit results. For example, the ratio of branching ratios $\mathrm{Br}(B \to D_2^* e\nu)/\mathrm{Br}(B \to D_1 e\nu)$ changes from the value of about 1.6 in the heavy quark limit, $m_Q \to \infty$, to the value of about 1 after subleading corrections are included.

In conclusion, we have presented here the first self-consistent dynamical calculation of subleading heavy quark corrections in the framework of the relativistic quark model, which are found to be in agreement with the HQET predictions.

ACKNOWLEDGMENTS

We thank D.V. Antonov, M. Beneke, J.G. Körner and V.I. Savrin for useful discussions. R.N.F. gratefully acknowledges the warm hospitality of the colleagues in the particle theory group of the Humboldt-University extended to him during his stay there. R.N.F and V.O.G. were supported in part by the *Deutsche Forschungsgemeinschaft* under contract Eb 139/1-3.

REFERENCES

[1] CLEO Collaboration, A. Anastassov *et al.*, Phys. Rev. Lett. **80**, 4127 (1998).
[2] ALEPH Collaboration, D. Buskulic *et al.*, Z. Phys. C **73**, 601 (1997).
[3] OPAL Collaboration, R. Akers *et al.*, Z. Phys. C **67**, 57 (1995).
[4] N. Isgur and M.B. Wise, Phys. Lett. B **232**, 113 (1989) and **237**, 527 (1990); M.B. Voloshin and M.A. Shifman, Sov. J. Nucl. Phys. **45**, 292 (1987) and **47**, 511 (1988).
[5] N. Isgur and M.B. Wise, Phys. Rev. D **43**, 819 (1991).
[6] A.K. Leibovich *et al.*, Phys. Rev. D **57**, 308 (1998).
[7] D. Ebert, V.O. Galkin and R.N. Faustov, Phys. Rev. D **57**, 5663 (1998) and **59**, 019902 (1999) (Erratum).
[8] R.N. Faustov, V.O. Galkin and A.Yu. Mishurov, Phys. Lett. B **356**, 516 (1995) and **367**, 391 (1996) (Erratum); Phys. Rev. D **53**, 6302 (1996); R.N. Faustov and V.O. Galkin, Phys. Rev. D **52**, 5131 (1995).
[9] D. Ebert, R.N. Faustov and V.O. Galkin, Phys. Rev. D **56**, 312 (1997).
[10] R.N. Faustov and V.O. Galkin, Z. Phys. C **66**, 119 (1995).
[11] D. Ebert, R.N. Faustov and V.O. Galkin, Phys. Lett. B **434**, 365 (1998).
[12] A.A. Logunov and A.N. Tavkhelidze, Nuovo Cimento **29**, 380 (1963).
[13] A.P. Martynenko and R.N. Faustov, Teor. Mat. Fiz. **64**, 179 (1985).
[14] V.O. Galkin, A.Yu. Mishurov and R.N. Faustov, Yad. Fiz. **55**, 2175 (1992) [Sov. J. Nucl. Phys. **55**, 1207 (1992)].
[15] D. Ebert, R.N. Faustov and V.O. Galkin, Eur. Phys. J. C **7**, 539 (1999).
[16] V.O. Galkin and R.N. Faustov, Yad. Fiz. **44**, 1575 (1986) [Sov. J. Nucl. Phys. **44**, 1023 (1986)]; V.O. Galkin, A.Yu. Mishurov and R.N. Faustov, Yad. Fiz. **51**, 1101 (1990) [Sov. J. Nucl. Phys. **51**, 705 (1990)].
[17] R.N. Faustov, Ann. Phys. **78**, 176 (1973); Nuovo Cimento A **69**, 37 (1970).
[18] S. Veseli and M.G. Olsson, Phys. Rev. D **54**, 886 (1996).
[19] V. Morénas *et al.*, Phys. Rev. D **56**, 5668 (1997).
[20] A. Deandrea *et al.*, Phys. Rev. D **58**, 034004 (1998).
[21] A. Wambach, Nucl. Phys. B **434**, 647 (1995).
[22] P. Colangelo, F. De Fazio and N. Paver, Phys. Rev. D **58**, 116005 (1998).
[23] S. Godfrey and N. Isgur, Phys. Rev. D **32**, 189 (1985).
[24] P. Colangelo, G. Nardulli and M. Pietroni, Phys. Rev. D **43**, 3002 (1991).
[25] J.D. Bjorken, in *Results and Perspectives in Particle Physics*, Proceedings of Les Recontres de la Vallée d'Aoste, La Thuile, Italy, 1990, edited by M. Greco (Editions Frontieres, Gif-sur-Yvette, France, 1990).
[26] C. Caso *et al.*, Particle Data Group, Eur. Phys. J. C **3**, 1 (1998).

TABLES

TABLE I. The comparison of our results for the values of the leading Isgur–Wise functions τ and ζ at zero recoil of the final D^{**} meson and their slopes ρ_j^2 with other predictions.

	Ours	[6]	[20]	[21]	[22]	[19], [23]	[19], [24]
$\tau(1)$	0.85	0.71	0.97	1.14		1.02	0.90
$\rho^2_{3/2}$	1.53	1.5	2.3	1.9		1.5	1.45
$\zeta(1)$	0.59	0.82	0.18	0.82	0.70 ± 0.16	0.44	0.12
$\rho^2_{1/2}$	1.04	1.0	1.1	1.4	2.5 ± 1.0	0.83	0.73

TABLE II. Decay rates Γ (in units of $|V_{cb}/0.04|^2 \times 10^{-15}$ GeV) and branching ratios BR (in %) for $B \to D^{**} e\nu$ decays in the infinitely heavy quark mass limit and taking account of first order $1/m_Q$ corrections. R is a ratio of branching ratios taking account of $1/m_Q$ corrections to branching ratios in the infinitely heavy quark mass limit.

	$m_Q \to \infty$		With $1/m_Q$			Experiment	
Decay	Γ	Br	Γ	Br	R	Br (CLEO) [1]	Br (ALEPH) [2]
$B \to D_1 e\nu$	1.4	0.32	2.7	0.63	1.97	$0.56 \pm 0.13 \pm 0.08 \pm 0.04$	0.74 ± 0.16
$B \to D_2^* e\nu$	2.1	0.51	2.5	0.59	1.16	< 0.8	< 0.2
$B \to D_1^* e\nu$	0.31	0.073	0.39	0.09	1.23		
$B \to D_0^* e\nu$	0.25	0.061	0.59	0.14	2.3		

TABLE III. Decay rates Γ (in units of $|V_{cb}/0.04|^2 \times 10^{-15}$ GeV) and branching ratios BR (in %) for $B \to D_s^{**} e\nu$ decays in the infinitely heavy quark mass limit and taking account of first order $1/m_Q$ corrections. R is a ratio of branching ratios taking account of $1/m_Q$ corrections to branching ratios in the infinitely heavy quark mass limit.

	$m_Q \to \infty$		With $1/m_Q$		
Decay	Γ	Br	Γ	Br	R
$B \to D_{s1} e\nu$	1.5	0.36	4.5	1.06	2.9
$B \to D_{s2}^* e\nu$	2.4	0.56	3.2	0.75	1.3
$B \to D_{s1}^* e\nu$	0.53	0.13	0.77	0.18	1.4
$B \to D_{s0}^* e\nu$	0.44	0.10	1.6	0.37	3.6

TABLE IV. Predictions for ratios of decay rates $B \to D_2^* e\nu$, $B \to D_0^* e\nu$, and $B \to D_1^* e\nu$ to the rate $B \to D_1 e\nu$ in the $m_Q \to \infty$ limit and taking account of $1/m_Q$ corrections. In the last line we show our predictions for the sum of branching ratios (in %) of B decays to orbitally excited D^{**} mesons.

	$m_Q \to \infty$	With $1/m_Q$
$\mathrm{Br}(B \to D_2^* e\nu)/\mathrm{Br}(B \to D_1 e\nu)$	1.59	0.94
$\mathrm{Br}(B \to D_0^* e\nu)/\mathrm{Br}(B \to D_1 e\nu)$	0.19	0.22
$\mathrm{Br}(B \to D_1^* e\nu)/\mathrm{Br}(B \to D_1 e\nu)$	0.23	0.14
$\sum \mathrm{Br}(B \to D^{**} e\nu)/\mathrm{Br}(B \to D_1 e\nu)$	3.0	2.3
$\sum \mathrm{Br}(B \to D^{**} e\nu)$	0.96	1.45

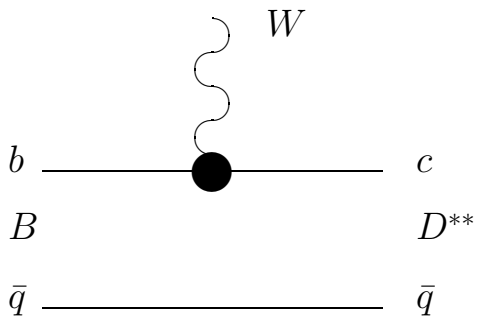

FIG. 1. Lowest order vertex function $\Gamma^{(1)}$ contributing to the current matrix element (18).

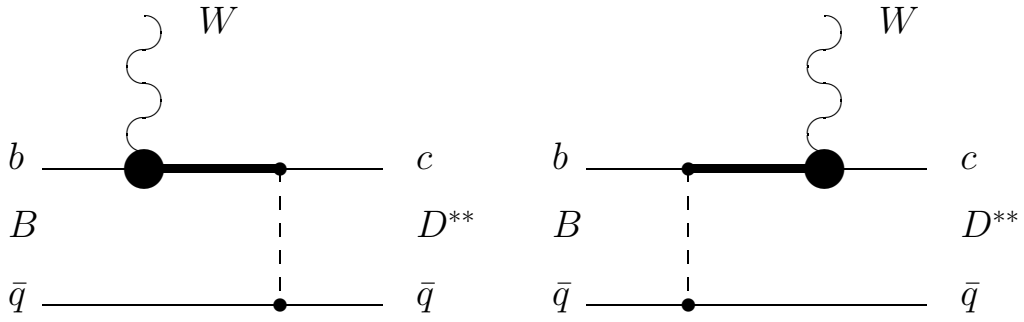

FIG. 2. Vertex function $\Gamma^{(2)}$ taking the quark interaction into account. Dashed lines correspond to the effective potential (12). Bold lines denote the negative-energy part of the quark propagator.

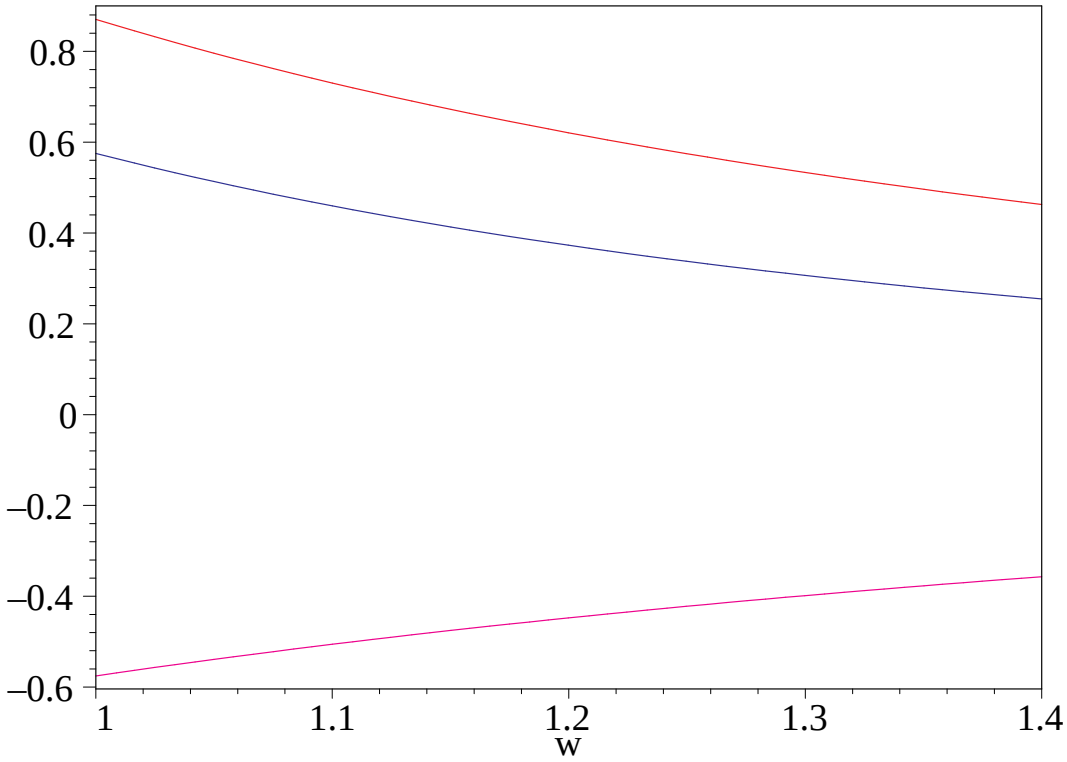

FIG. 3. Isgur–Wise functions $\tau(w)$ (upper curve), $\tau_1(w)$ (middle curve) and $\tau_2(w)$ (lower curve) for the $B \to D_{1,2} e\nu$ decay.

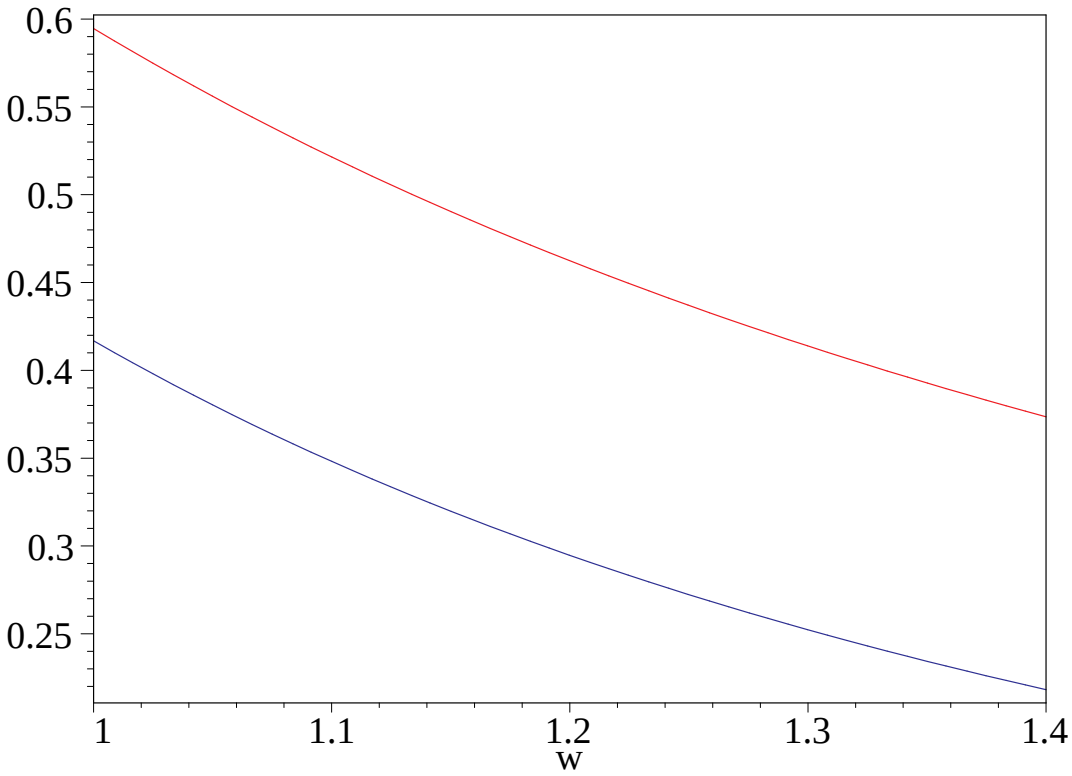

FIG. 4. Isgur–Wise functions $\zeta(w)$ (upper curve) and $\zeta_1(w)$ (lower curve) for the $B \to D^*_{0,1} e\nu$ decay.

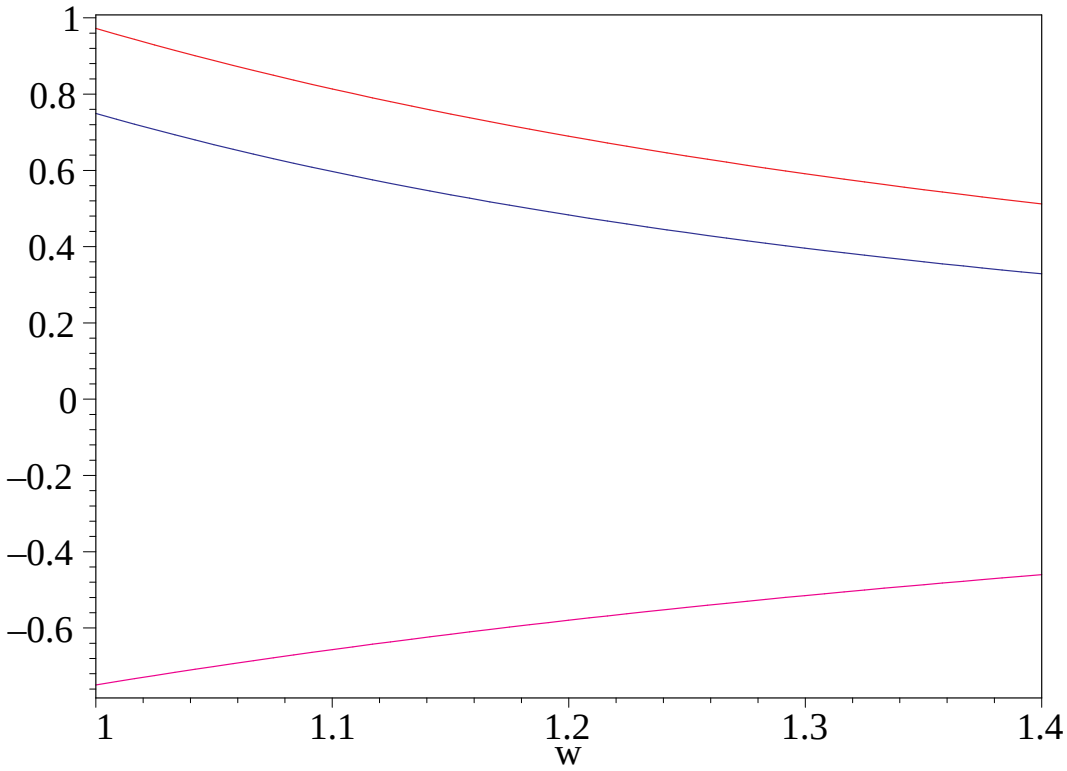

FIG. 5. Isgur–Wise functions $\tau(w)$ (upper curve), $\tau_1(w)$ (middle curve) and $\tau_2(w)$ (lower curve) for the $B_s \to D_{s1,2} e\nu$ decay.

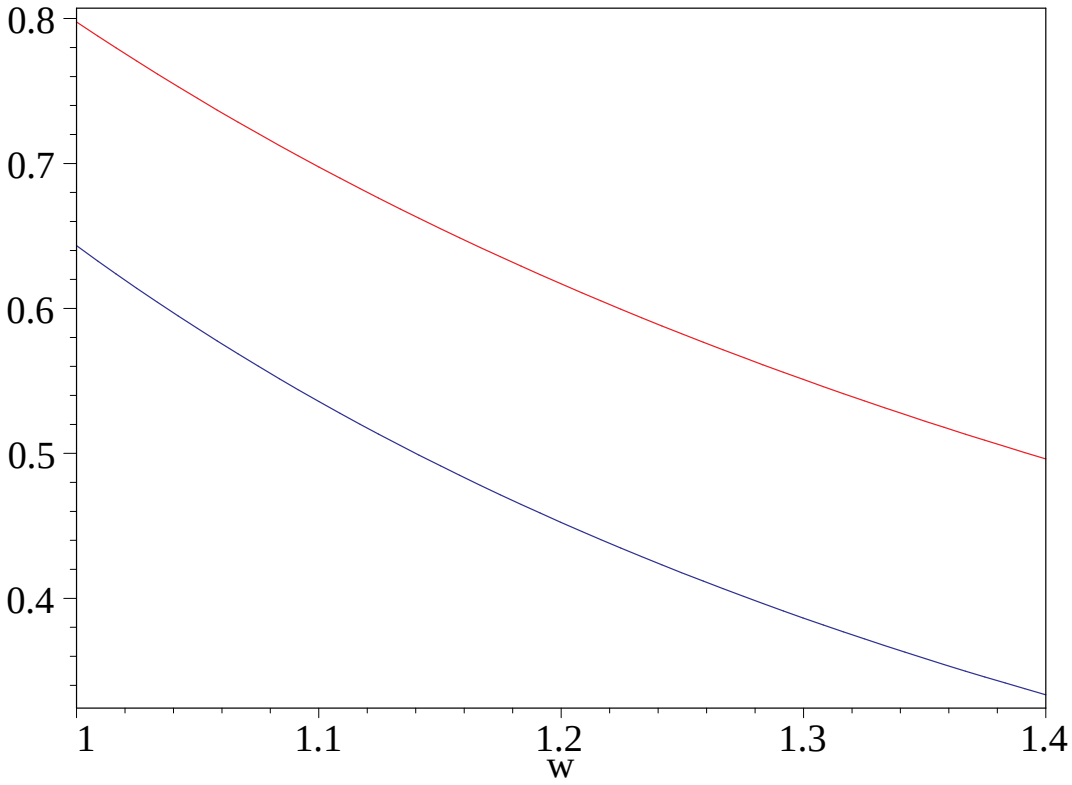

FIG. 6. Isgur–Wise functions $\zeta(w)$ (upper curve) and $\zeta_1(w)$ (lower curve) for the $B_s \to D^*_{s0,1} e\nu$ decay.

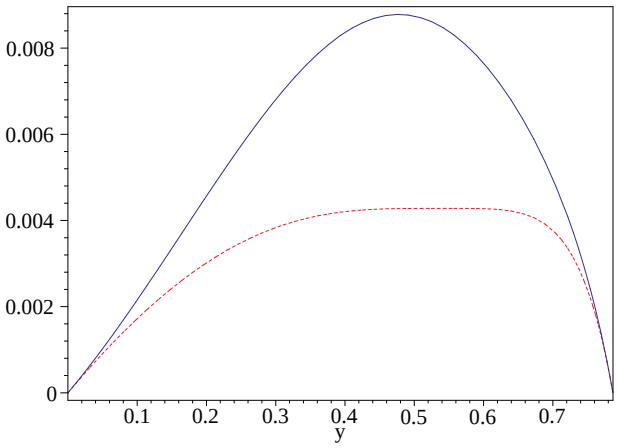

(a) $B \to D_0^* e\nu$

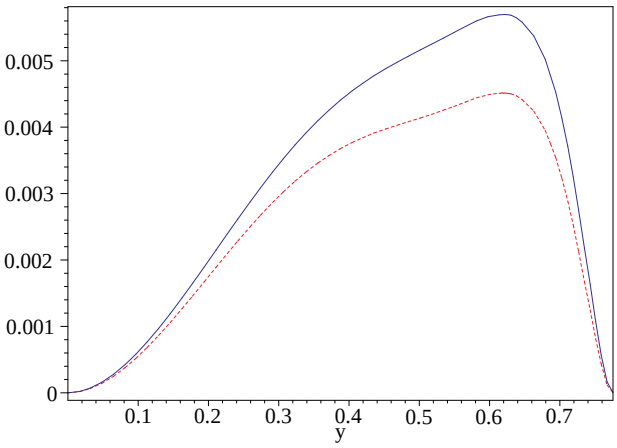

(b) $B \to D_1^* e\nu$

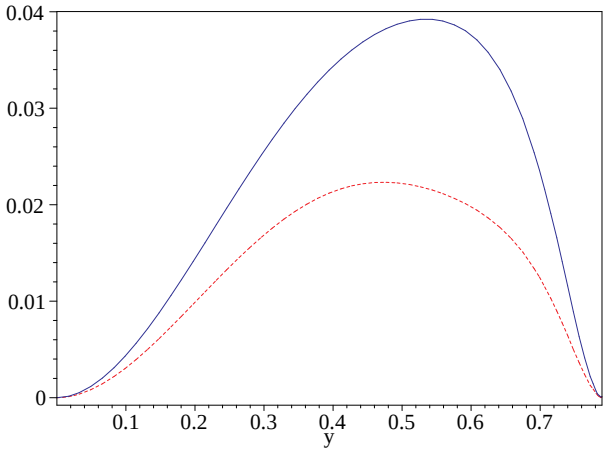

(c) $B \to D_1 e\nu$

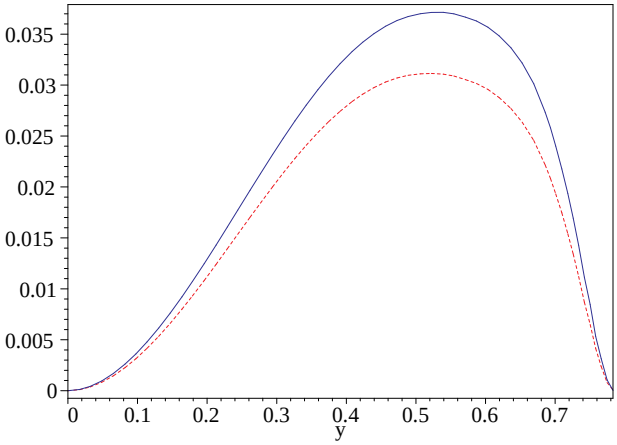

(d) $B \to D_2^* e\nu$

FIG. 7. Electron spectra $(1/\Gamma_0)\,(\mathrm{d}\Gamma/\mathrm{d}y)$ for the $B \to D^{**} e\nu$ decays. Dashed curves show the $m_Q \to \infty$ limit, solid curves include first order $1/m_Q$ corrections.